Mice With a Combined Deficiency of Superoxide Dismutase 1 (*Sod1*), DJ-1 (*Park7*), and Parkin (*Prkn*) Develop Spontaneous Retinal Degeneration With Aging

Yuanfei Zhu,* Bogale Aredo, Bo Chen,† Cynthia X. Zhao, Yu-Guang He, and Rafael L. Ufret-Vincenty

Department of Ophthalmology, UT Southwestern Medical Center, Dallas, Texas, United States

Correspondence: Rafael L. Ufret-Vincenty, Department of Ophthalmology, UT Southwestern Medical Center, 5323 Harry Hines Boulevard, Dallas, TX 75390-9057, USA; Rafael.Ufret-Vincenty@UTSouthwestern.edu.

YZ, BA, and BC contributed equally to the work presented here and should therefore be regarded as equivalent authors.

Current affiliation: *Shenzhen Eye Hospital, Shenzhen Key Laboratory of Ophthalmology, Shenzhen University School of Medicine, Shenzhen, Guangdong, China. †Department of Ophthalmology, Tongji Hospital, Tongji Medical College, Huazhong University of Science and Technology, Wuhan, Hubei Province, China.

Submitted: April 1, 2019
Accepted: June 28, 2019

Citation: Zhu Y, Aredo B, Chen B, Zhao CX, He Y-G, Ufret-Vincenty RL. Mice with a combined deficiency of superoxide dismutase 1 (*Sod1*), DJ-1 (*Park7*), and Parkin (*Prkn*) develop spontaneous retinal degeneration with aging. *Invest Ophthalmol Vis Sci*. 2019;60:3740–3751. https://doi.org/10.1167/iovs.19-27212

Purpose. Chronic oxidative stress is an important mechanism of disease in aging disorders. We do not have a good model to recapitulate AMD and other retinal disorders in which chronic oxidative stress plays an important role. We hypothesized that mice with a combined deficiency in superoxide dismutase 1 (*Sod1*), DJ-1 (*Park-7*), and Parkin (*Prkn*) (triple knock out, TKO) would have an increased level of chronic oxidative stress in the retina, with anatomic and functional consequences just with aging.

Methods. Eyes of TKO and B6J control mice were (1) monitored with optical coherence tomography (OCT) and electroretinography (ERG) over time, and (2) collected for oxidative marker protein analysis by ELISA or immunohistochemistry and for transmission electron microscopy studies.

Results. TKO mice developed qualitative disruptions in outer retinal layers in OCT by 3 months, increased accumulation of fundus spots and subretinal microglia by 6 months of age, significant retinal thinning by 9 months, and decreased ERG signal by 12 months. Furthermore, we found increased accumulation of the oxidative marker malondialdehyde (MDA) in the retina and increased basal laminal deposits (BLD) and mitochondria number and size in the retinal pigment epithelium of aging TKO mice.

Conclusions. TKO mice can serve as a platform to study retinal diseases that involve chronic oxidative stress, including macular degeneration, retinal detachment, and ischemic retinopathies. In order to model each of these diseases, additional disease-specific catalysts or triggers could be superimposed onto the TKO mice. Such studies could provide better insight into disease mechanisms and perhaps lead to new therapeutic approaches.

Keywords: aging; age-related macular degeneration, superoxide dismutase 1, *Sod1*, DJ-1, *Park7*, Parkin, *Prkn*, oxidative stress

Oxidative stress is widely recognized as an important mechanism of disease in aging disorders, including those affecting the retina and the nervous system. Among the many disorders known to have a significant oxidative stress component, prevalent ones include AMD,[1–7] retinal dystrophies,[8] and neurodegenerative diseases, such as Alzheimer's and Parkinson's disease.[9]

Cells are equipped with endogenous antioxidant defense mechanisms, which respond, interact, and protect against the damaging effects of oxidative stress, including superoxide dismutase 1 (*Sod1* gene), Parkin (*Prkn* or *Park2* gene), and DJ-1 (*Park7* gene). These three proteins have been shown to be active in the retina and to regulate oxidative stress in the retinal environment.[10–15] DJ-1 has been found to be very important in protecting photoreceptors and retinal pigment epithelium (RPE) cells from oxidative damage during aging[11] and in response to a systemic challenge with an oxidizing agent (sodium iodate).[10] It has been demonstrated that DJ-1 is increased in RPE cells in culture after an oxidative stressor is applied, and that DJ-1 is elevated in the RPE of AMD patients.[15] Prior studies have found that Sod1 is essential in protecting the retina from oxidative stress induced by paraquat and hyperoxia,[12] and by aging.[14] Parkin has also been shown to be present in the retina of humans,[13] and has been found to play an important role in the response of cells to oxidative stress[16–18] and in the protection of retinal ganglion cells against glutamate excitotoxicity.[19] Recognizing that single knock-out (KO) mice (*Sod1* KO mice, DJ-*1* [*Park7*] KO mice, and Parkin [*Prkn*] KO mice) have been shown to develop retinal changes with aging, we wanted to determine if mice simultaneously deficient in all three genes would represent an additional model for oxidative stress–related retinal disease that would add to our current models.

It has been reported that DJ-1 can regulate Sod1 expression through the ERK1/2-ELK1 pathways, and that there is an upregulation of DJ-1 protein levels in mutant *Sod1* transgenic mice.[20,21] DJ-1 forms complexes with mutant Sod1 molecules and reduces the toxicity of the latter to tissues.[21] This suggests that a compensatory mechanism may reduce the likelihood of a clinical outcome when studying single loss-of-function mutations, at least in low-stress conditions. This is demonstrated by the lack of prominent neuropathology and age-related deficits in mice with targeted mutations of Parkin or DJ-1 with normal aging, despite the fact that progressive neurodegeneration is seen in these mice upon exposure to external stressors (reviewed in Hennis et al.).[22] Interestingly previous studies in the central nervous system reported a lack of progressive loss of dopaminergic neurons in mice simultaneously deficient in *Sod1/Park7/Prkn* (triple KO [TKO] mice).[22] However, we hypothesized that due to the fact that the retina is a pro-oxidant environment, *Sod1/Park7/Prkn* TKO mice will demonstrate early development of AMD-like features under normal aging conditions.

We have previously shown that Sod1/DJ-1/Parkin (here referred to as *Sod1/Park7/Prkn*) TKO mice have increased susceptibility to light-induced retinal damage.[23] In the current study, we report that, with normal aging, these TKO mice develop qualitatively abnormal morphology on OCT as early as 3 to 6 months of age, followed by quantitatively thinner retinas on OCT by 9 months of age, and finally decreased retinal function on electroretinography (ERG). As early as 6 months of age they also demonstrate a very significant accumulation of fundus spots (which appear to correlate with Iba-1+ microglia). ELISA of retinal protein isolates and immunohistochemistry of retinal sections revealed an increase in the retinal levels of the oxidative marker, MDA. We also show an increased number and size of RPE mitochondria and increased accumulation of basal laminar deposits (BLD). Our results suggest that the TKO mice are a good model of chronic retinal oxidative stress. More importantly, we believe that these mice could prove particularly helpful in generating more AMD-like models when combined with other genetic or chronic environmental risk factors in combination with aging.

Methods

Animals and Genotyping of Mice

All animal experiments complied with the National Institutes of Health guide for the care and use of Laboratory animals and the ARVO Statement for the Use of Animals in Ophthalmic and Vision Research. All procedures were approved by the UT Southwestern Medical Center (UTSW) Institutional Animal Care and Use Committee (IACUC, Protocol # 2015-G100937). *Sod1/Park7/Prkn* KO mice (TKO)[23] were kindly provided by Matthew Goldberg, PhD. KO lines had been backcrossed to C57BL/6J mice for 10 generations without testing for the RD8 mutation (personal communication: Matthew Goldberg 2013). However, upon receiving the mice, genotyping and sequencing for the Rd8 mutation of the *Crb1* gene[24,25] revealed some expression of this mutation in the KO lines. The lines were thus back-crossed to C57BL/6J mice for three generations and then intercrossed to generate *Sod1/Park7/Prkn* TKO mice. From the early stages of this breeding, littermates heterozygous for the alleles were intercrossed to generate mice homozygous for the wild-type copies of *Sod1*, *Park7*, *and Prkn*. These were then interbred to generate a line of "B6 controls" for the rest of the TKO experiments. Further genotyping and sequencing confirmed the absence of the Rd8 mutation in the resulting "TKO" and "B6 control" lines of mice. Age- and sex-matched TKO and B6 control mice were aged to 3, 6, 9, 12, and 15 months. Between 16 and 18 months of age, TKO mice started developing corneal opacification and neovascularization (Supplementary Fig. S1) and began dying. The shortened life span of mouse models of increased oxidative stress is not uncommon.[26,27] Because these issues made cohorts above 16 months of age unusable for most experiments, we decided to terminate all experiments at 15 to 16 months of age. Mice were bred and kept in a barrier animal facility at UTSW under normal lighting conditions with 12-hour on/12-hour off cycles with free access to food and water. Before performing all procedures, mice were anesthetized with a ketamine-xylazine cocktail (100 mg/kg ketamine, 5 mg/kg xylazine) one at a time. Mouse eyes were dilated using one drop per eye of a mixture (1:1) of tropicamide 1% solution (Alcon Laboratories, Inc., Fort Worth, TX, USA) and phenylephrine hydrochloride 2.5% solution (Alcon, Inc., Lake Forest, IL, USA).

Image-Guided OCT, Retinal Layer Thickness Measurement, and Outer Retinal Reflectivity Assessment

Mice were anesthetized one at a time, and pupils were dilated. GenTeal liquid gel (Novartis, East Hanover, NJ, USA) was applied to the corneal surface. OCT images were taken using an image-guided tomographer (Micron IV-OCT2; Phoenix Research Laboratories, Pleasanton, CA, USA). For retinal layer thickness measurement, a short (half size), horizontal line was placed 1-disc diameter superior to the edge of the disc. For quantitative assessment of retinal layer thickness at the target location we used the Freehand tool in ImageJ (http://imagej.nih.gov/ij/; provided in the public domain by the National Institutes of Health, Bethesda, MD, USA). Three measurements were taken 200 μm apart in the center of the image for each of the measured parameters as follows: outer nuclear layer (ONL), external limiting membrane-Bruch's membrane (ELM-BM), and total retina thickness (internal limiting membrane-BM [ILM-BM]). Finally, the data for each image/eye were averaged for statistical analysis.

For the quantitative assessment of the outer retinal reflectivity we used a modification of a method we previously published.[28] The Freehand tool in ImageJ was used to delineate first the outer segment band and then the ellipsoid zone in OCT images in order to determine the mean intensity of each of these areas. We then defined the relative outer retina reflectivity (RORR) as the ratio of the mean intensity of the outer segments to the mean intensity of the ellipsoid zone. Finally, we normalized the values to those of B6 controls and reported the result as the normalized RORR (nRORR). This analysis was only done for mice up to 6 months of age, because by 9 months of age there was too much disruption of the outer retinal layers to allow for a reliable measurement of nRORR.

Fundus Photography and Spots Grading System

Fundus photographs of mice were obtained using a Micron IV mouse fundus camera (Phoenix Research Laboratories) as described before.[29] Briefly, a fundus image of each eye, centered on the optic nerve head, was obtained after sharply focusing on the RPE. Images from each experiment were saved and masked for fundus spot grading in a blind fashion. We used a modified version of a fundus spot scale, which was described previously[1] to categorize the amount of fundus spots in each image. Briefly, a fundus spot score for each eye is determined based on the amount of white/yellow fundus spots present as follows: no spots (score 0), 1 to 10 fundus spots (score 1), equivalent of one fundus-quadrant of spots (score 2), two to three fundus-quadrants of spots (score 3), and all four fundus-

Investigative Ophthalmology & Visual Science

quadrants with spots (score 4). We then added the scores of both eyes for a final score of 0 to 8 for each mouse. Because this is an ordinal discrete variable, statistical analysis for comparisons between B6 and TKO was done using a Mann-Whitney *U* test.

Electroretinography

ERG responses were recorded in dark-adapted TKO mice and in age- and sex-matched B6 control mice at 6, 12, and 15 months of age using a Ganzfeld scotopic ERG system (Phoenix Research Labs) as stated by the company. Briefly, mice were dark-adapted overnight for 16 hours. After anesthesia and pupil dilation, mice were placed on a platform covered by a homeothermic heating blanket to maintain body temperature, and preparations were made under a dim red light. GenTeal liquid gel was applied to each eye after anesthesia to prevent corneal drying (left eye) and to establish contact between the cornea and the electrode (gold-plate objective lens; right eye). The reference and the ground electrodes (platinum needles) were subcutaneously inserted on top of the head and into the tail, respectively. Scotopic full-field ERGs were obtained in response to low- (0.1 log cd.s.m^{-2}) and high- (3.1 log cd.s.m^{-2}) flash intensities (the interstimulus interval was 0.7 and 60 seconds for low- and high-flash intensities, respectively; flash duration was 1 msec). For scotopic ERG analysis, the amplitude of the a-wave was measured from baseline to the most negative trough, whereas that of the b-wave was measured from the trough of the a-wave to the most positive peak of the retinal response.

RPE Flat-Mount Preparation and Immunostaining

After marking the superior aspect of the cornea for orientation, eyes were enucleated from deeply anesthetized 15-month-old TKO mice and age-matched B6 control mice of both sexes. The anterior segment (cornea, iris, and lens) was removed by cutting around the limbus, and the retina was peeled away from the RPE–choroid for MDA–ELISA assay (see below). After making our six radial cuts from the edge to the center, the remaining RPE–choroid–sclera eyecups (flat mounts) were then fixed in 4% paraformaldehyde for 30 minutes at room temperature, followed by 3 × 10-minute washes in 1× PBS. The eyecups were then incubated in blocking buffer (5% BSA, 0.3% Triton X-100) for 2 hours at room temperature (RT) on a rocking shaker. The flat mounts were incubated in anti-MDA and anti-Iba-1 primary antibodies diluted in 1% BSA, 0.3% Triton X-100 (dilutions: anti-MDA, 1:100; anti-Iba-1 1:500) overnight at 4°C on a rocking shaker. After washing 3 × 10 minutes in 1× PBS, the tissues were incubated with appropriate secondary antibodies and fluorescently labeled Phalloidin antibody (diluted in 1% BSA, 0.3% Triton X-100) for 2 hours at RT on a rocking shaker. Following 3 × 10-minute washes in 1× PBS, the tissues were placed with the RPE facing up on glass slides using mounting medium with 4′,6-diamidino-2-phenylindole (DAPI). A coverslip was carefully placed (trying to minimize trapped air bubbles), resulting in the RPE flat mount. The flat mounts were photographed with a Leica TCS SP8 confocal laser scanning microscope (Leica Microsystems Inc., Buffalo Grove, IL, USA) using a water immersion objective at ×25 magnification. Twelve images (4 central superior, 4 central inferior, and 4 peripheral) were taken per flat mount. A total count for Iba-1+ cells and also for MDA+/Iba-1+ cells was obtained for each flat mount by adding the counts for all 12 images. The average of these total counts for all B6 control flat mounts was then compared with the average for all TKO flat mounts.

Protein Isolation From Mouse Retina for MDA ELISA

After enucleation, the posterior eyecups were immediately dissected out for protein isolation to run quantitative MDA ELISA as described before.[1] Briefly, the retina was separated and homogenized in 120-µL T-PER tissue protein extraction reagent (catalog No. 78510; Thermo Scientific, Rockford, IL, USA) containing a protease inhibitor cocktail. The homogenate was centrifuged at 10,000*g* for 20 minutes at 4°C and the supernatant was transferred to a new tube. Protein concentration was determined by NanoDrop ND-1000 UV/Vis spectrophotometer (NanoDrop Technologies, Wilmington, DE, USA). The OxiSelect MDA-Adduct Competitive ELISA Kit (catalog No. STA-832; Cell Biolabs, Inc., San Diego, CA, USA) was used to determine the MDA–protein complex content in the retinal samples according to the kit's protocol. Absorbance of each well was read on a BioTek Synergy2 microplate reader (BioTek Instruments, Inc., Winooski, VT, USA) at 450 nm. Samples were run in duplicates.

Immunohistochemistry of Retinal Sections

One eye of each mouse ($n = 4$ per group) was enucleated for freeze substitution as described before[30] and the other eye was collected for electron microscopy (see below). Freeze substituted eyes were transferred to ethanol for routine paraffin embedding.[30] Retinal sections (5 µm) were deparaffinized, blocked, and incubated overnight at 4°C in anti-MDA primary antibody (LS-C72018: rabbit ant-MDA, 1:200; LifeSpan Biosciences, Inc., city, state, country), followed by incubation for 2 hours in a secondary antibody conjugated to AF488 (A21206: donkey anti-rabbit, 1:200; Life Technologies, Seattle, WA, USA). Fluorescence staining was visualized and Z-stack images of the retina were taken with a Leica TCS confocal laser-scanning microscope equipped with LAS X, a Leica Application Suite (Leica Microsystems, Inc.) using a ×25 water immersion objective.

Electron Microscopy Imaging and Analyses

Sample Processing and Transmission Electron Microscopy. Mice were perfused through the heart with 2% glutaraldehyde and 2% paraformaldehyde in PBS (pH 7.4). The eyes were removed and sectioned behind the limbus, and posterior eyecups were processed as described before.[29] For electron microscopy, thin sections (70 nm) were cut and stained with 2% aqueous uranyl acetate and lead citrate (UTSW Electron Microscopy Core). The thin sections were imaged with JEOL JEM 1200EX transmission electron microscope (JEOL USA, Inc., Peabody, MA, USA) equipped with a tungsten source at 120 kV using a Morada SIS camera (Olympus, Munster, Germany). The images were analyzed for the number of mitochondria, the area of the mitochondria and the amount of BLD under the RPE by masked investigators using ImageJ software.

Mitochondrial Counting and BLD Measurement. Transmission electron microscopy (TEM) images were opened in ImageJ software for quantitative analysis. In order to determine the number of mitochondria, a line was drawn horizontally, splitting the RPE cells into basal and apical halves. Mitochondria were counted on either side of the line and labeled as basal or apical. All mitochondria that touched the line were classified and counted as "mid-RPE." We also reported the addition of basal, apical, and "mid-RPE" mitochondria as "total mitochondria." For quantification of the BLD, the total area of BLD accumulation was measured using the freehand tracing tool in ImageJ. This number was divided by the length of the RPE

Investigative Ophthalmology & Visual Science

measured in order to normalize for the total amount of tissue measured in each image. The ratio is reported as BLD standard units (SU).

Statistical Analysis

SigmaPlot 11.0 (Systat Software, Inc., San Jose, CA, USA) was used for statistical analysis. Data are presented as the mean ± SEM. A two-tailed Student's *t*-test or the Mann-Whitney *U* test was performed when comparing two groups. A P value < 0.05 was considered to be statistically significant.

Results

Retinal Degeneration Can Be Quantified Using OCT Analysis of the Retinal Layers and is More Pronounced in Aging TKO Mice

In order to determine whether the chronic increase in oxidative stress in TKO mice had an impact on their retinal anatomy, and to evaluate the time course of that effect we decided to obtain OCT images of TKO and B6 control mice at different ages. First, we made qualitative comparisons of OCT images based on the integrity of retinal layers between the two groups (Fig. 1). We found that by 3 months of age, we could consistently find in TKO mice an increase in reflectivity of the photoreceptor outer segment layer (see white arrowheads in Figs. 1F versus 1B, and 1E versus 1A). In order to quantitate changes in reflectivity of the outer retina we had previously compared the mean intensity of the photoreceptor outer segments with that of the ellipsoid zone.[28] We now call this parameter RORR. TKO mice showed by 3 months of age a statistically significant increase in RORR compared with B6 controls (Fig. 1I; $P = 1 \times 10^{-5}$ for 3 months and $P = 7 \times 10^{-4}$ for 6 months). Furthermore, progressive disruption of the outer retinal layers was seen by 9 months of age, with thinning of the outer segments, loss of the interdigitation zone, and visible thinning of the retina outside the ellipsoid zone (compare the thickness and appearance of the layers encompassed by the white brackets in Fig. 1G versus 1C).

Quantitative analysis was then performed. The OCT images were analyzed by measuring the distance between BM and the ELM (BM_ELM; Fig. 2A), between the ELM and the innermost aspect of the ONL (ELM_ONL; Fig. 2B) and between BM and the ILM (BM_ILM or total retinal thickness; Fig. 2C). For the most part, the OCT images did not reveal a significant difference in thickness between TKO and B6 control mice up until 6 months of age. However, by 9 months of age there was a statistically significant decrease in retinal thickness (*P* values for BM_ELM, ELM_ONL and BM_ILM were 0.026, 0.0085, and 0.0077, respectively) in TKO mice compared with B6 control mice. This retinal thinning in TKO mice was worse by 15 months of age (corresponding *P* values were 0.000005, 0.0004, and 0.0024).

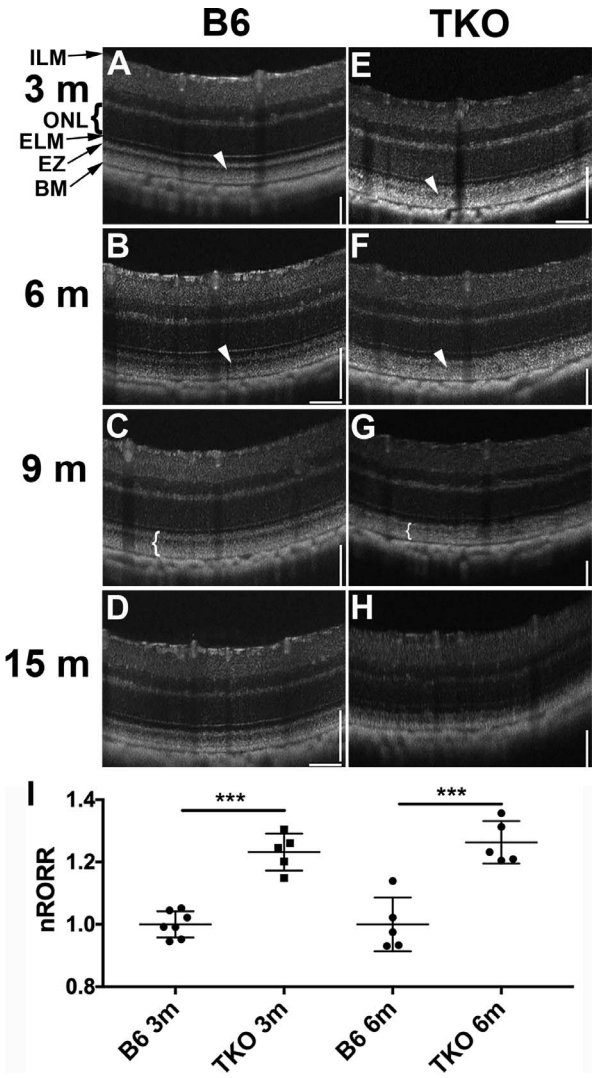

Figure 1. Outer retinal abnormalities are seen in TKO mice by 3 months of age. OCT images of B6 control mice are shown at 3 (**A**), 6 (**B**), 9 (**C**), and 15 months (**D**). Representative OCT images of TKO mice at 3 (**E**), 6 (**F**), 9 months (**G**) and 15 months (**H**) are also shown. Hyperreflectivity of the outer retina, external to the ellipsoid zone is seen consistently by 6 months of age in TKO mice, but not in B6 controls (*white arrowheads* in **F** versus **B**). Outer retinal thinning and loss of the interdigitation zone and photoreceptor outer segments is seen as early as 9 months of age in TKO mice, but not in B6 controls (compare the thickness and appearance of the layers encompassed by the *white brackets* in **G** versus **C**). Quantification of the reflectivity changes was done using the parameter RORR ([mean intensity of the photoreceptor outer segments]/[mean intensity of the ellipsoid zone]). Each mean intensity was determined using ImageJ. Finally, we normalized the values to those of B6 controls and reported the result as the nRORR (**I**). $^{***}P < 0.001$.

Accumulation of Fundus Spots and Subretinal Microglia/Macrophages in Aging TKO Mice

We have previously described that TKO mice (*Sod1*$^{-/-}$, *DJ-1*$^{-/-}$, *Parkin*$^{-/-}$) demonstrate increased susceptibility to acute oxidative stress in a light injury model.[23] In the current study, we explore the effect of chronic oxidative stress due to aging in the retinas of these mice. Upon clinical examination, the most obvious difference between TKO mice and age- and sex-matched B6 control mice is the accumulation of white/yellowish fundus spots in the TKO mice (Fig. 3). The difference becomes significant at approximately 5 to 6 months of age (Fig. 3B versus 3G, 3K; $P = 0.02$ at 6 months). Although there is some increase in the number of these fundus spots with age in both TKO and B6 control mice, the difference between the two groups increases with time (Fig. 3K; $P = 0.002$ at 9 months and $P = 2 \times 10^{-9}$ at 12 months). In fact, by 9 months of age these spots are covering the entire fundus of TKO mice (Fig. 3C versus 3H).

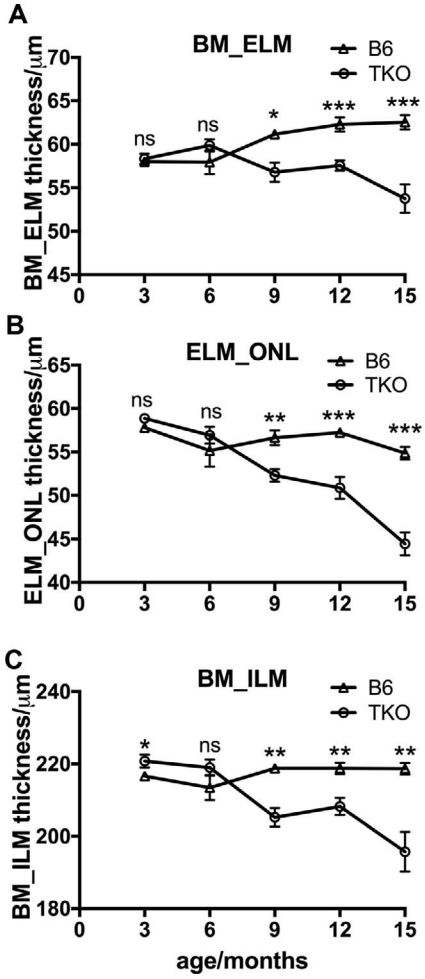

Figure 2. TKO mice demonstrate retinal thinning with aging. OCT images of TKO mice and age- and sex-matched B6 controls were obtained at 3, 6, 9, 12, and 15 months of age. The following parameters were measured: (**A**) distance from BM_ELM, (**B**) distance from the ELM_ONL, and (**C**) distance from BM_ILM. Compared with B6 control mice, TKO mice demonstrate significant thinning of the retina starting at 9 months of age. The decrease in BM_ELM, ELM_ONL, and BM_ILM continues to increase as the mice age. Each *symbol* represents mean values ± SEM for experimental groups. The following number of mice were analyzed for the 3-, 6-, 9-, 12-, and 15-month time points for each experimental group: B6 control = 15, 16, 3, 7, and 9, respectively; TKO = 12, 8, 5, 7, and 12, respectively. The statistical significance was reported as ns = no significant difference, $^{*}P < 0.05$, $^{**}P < 0.01$, $^{***}P < 0.001$.

Aging Leads to Increased Numbers of Iba-1+, and Malondialdehyde-Staining (MDA+) Subretinal Microglia in *Sod1/Park7/Prkn* TKO Mice

We and others have previously shown that the observed fundus spots correspond to subretinal microglia/macrophages.[1,24,29–32] In fact, we have previously found an almost 1:1 association between the number of Iba-1+ subretinal microglia in flat mounts and the number of fundus spots.[30] OCT imaging through these spots demonstrates that they correspond to hyperreflective spots that are external to the ellipsoid zone (Fig. 4), consistent with subretinal microglia. We wanted to confirm that the increasing number of fundus spots in TKO mice correlated with an increasing number of subretinal microglia. Moreover, we decided to test the hypothesis that the subretinal microglia in TKO mice may be associated with, and

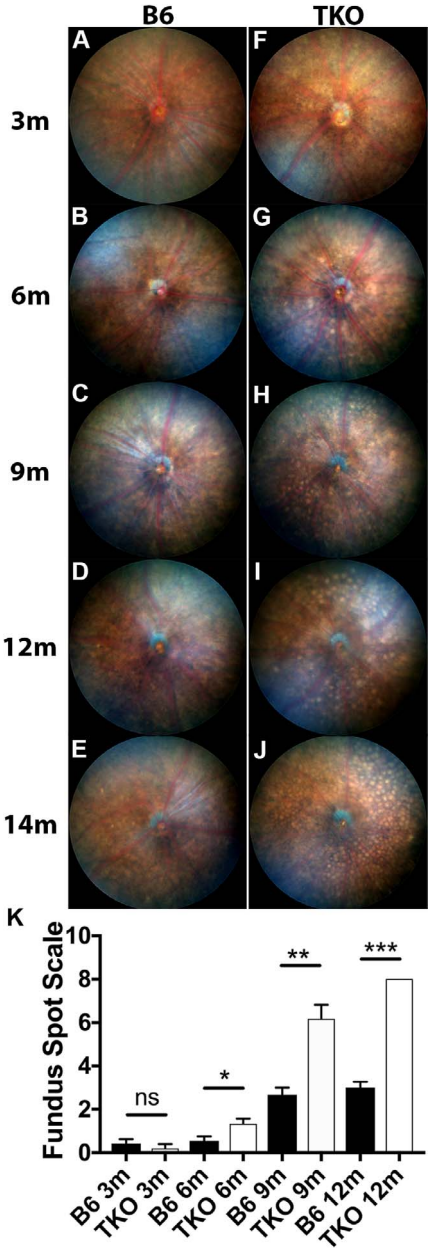

Figure 3. Increased fundus spots with aging in mice simultaneously deficient in Sod1/Park7/Prkn (TKO). While B6 control mice only have a few white/yellow fundus spots visible on fundus photos (**A–E**), TKO mice demonstrate a progressive accumulation of these spots with aging (**F–J**). The difference between TKO mice and B6 controls becomes statistically significant at 6 months of age and continues to increase (**K**). By 9 months of age the entire fundus is involved in the TKO mice (**H**). The scale used to grade the fundus spots is described in the Methods section. The following number of mice were scored for each time point: at 3 months, seven B6 controls and five TKO; at 6 months, 11 B6 controls and nine TKO; at 9 months, six B6 controls and six TKO; and at 12 months, eight B6 controls and eight TKO. *Error bars* represent the standard error of the mean for experimental groups. The statistical significance was reported as $^{*}P < 0.05$, $^{**}P < 0.01$, $^{***}P < 0.001$.

provide evidence for, an increased level of oxidative stress in the outer retina of these mice. To this end, we prepared RPE–choroid–scleral flat mounts from TKO and age-matched B6 control mice, and double stained for Iba-1 and MDA (see methods for details on the staining and analysis). In B6 control

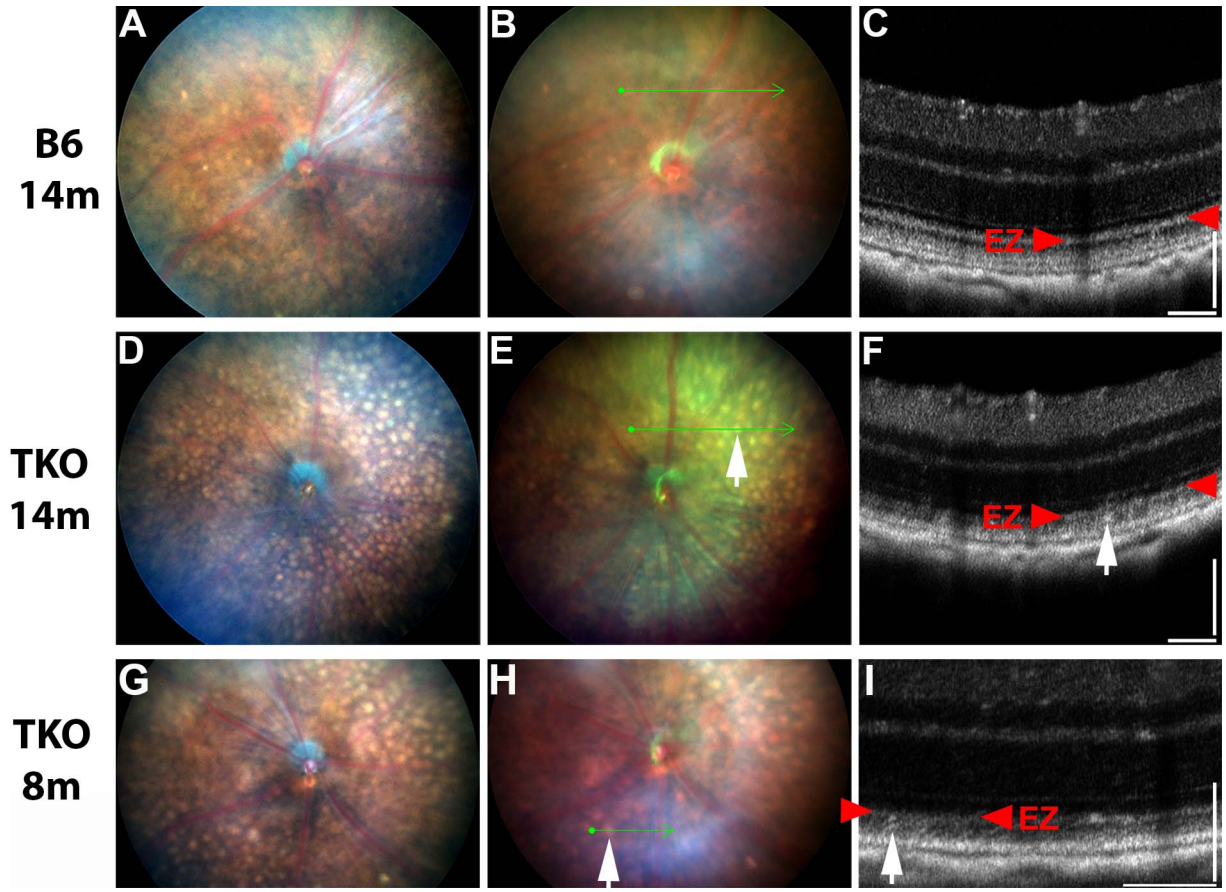

Figure 4. Fundus spots in photos and OCT images from 8- or 14-month B6 control and TKO mice. B6 control fundus photos showed very few yellow spots in the posterior fundus and normal retina layer reflectivity on OCT (**A–C**). TKO fundus photos demonstrate many fundus spots in all four quadrants (**D**, **E**, **G**, **H**) and focal areas of hyperreflectivity external to the ellipsoid zone (EZ) on OCT (**F**, **I**). *White arrows* show fundus spots on the fundus photos and the corresponding hyperreflective spots on OCT of the same TKO retinas. *Red arrowheads* label EZ on OCT images.

mice, we found very few ramified microglia overlying the RPE cells (Figs. 5A–C). In the meantime, large numbers of Iba-1+, MDA+ microglia agglomerated in age-matched TKO mice (Figs. 5D–F). Quantification of both Iba-1+ (Fig. 5G) and Iba-1+/MDA+ (Fig. 5H) cells on flat mounts demonstrated a statistically significant increase in aging TKO mice when compared with age-matched B6 control mice ($P = 0.0062$ for Iba-1+ and $P = 0.014$ for Iba-1+/MDA+).

MDA-Protein Adducts is Increased in the Retinas of Aging TKO Mice

Oxidative stress leads to lipid peroxidation, resulting in the accumulation of reactive compounds, such as MDA, which are then able to induce protein modification and damage. We assessed for MDA-protein adducts in the retinas of aging TKO and B6 control mice using immunohistochemistry and ELISA. Retina samples were collected from 13- to 16-month-old TKO and age- and sex-matched B6 control mice. We found an increased accumulation of MDA in the aging TKO mice by immunohistochemistry in retinal sections (Figs. 6A, 6B versus 6C, 6D). In the retina samples that were collected for ELISA, total protein was isolated and the concentration of MDA-protein adducts was determined using a commercial ELISA kit as described before[1] (Oxiselect MDA adduct competitive ELISA Kit; Cell Biolabs, Inc.). We found a statistically significant increase in MDA-protein adducts in TKO retinas compared with B6 controls (Fig. 6E, $P = 0.00058$).

Ultrastructural Changes in RPE of TKO Mice

Based on our observations of anatomic changes predominantly affecting the outer retina of TKO mice seen on OCT, we decided to also characterize the RPE changes in these mice. Eyes were collected from 15-month-old TKO and B6 control mice for TEM. The accumulation of BLD under the RPE was measured and found to be increased in aged TKO mice compared with age-and sex-matched B6 controls (Figs. 7A–C, $P = 0.0025$). We also analyzed the number of RPE mitochondria in all electron micrographs (×5000 magnification) from three B6 control eyes ($n = 120$ electron microscopy [EM] fields) and four TKO eyes ($n = 127$ EM fields). Others have measured the number of mitochondria in thin sections before.[33–36] This analysis demonstrated that the number of mitochondria was increased in TKO mice compared with B6 controls (Figs. 8A–E; total mitochondria, $P = 0.003$, apical mitochondria, $P = 0.0043$; basal mitochondria, $P = 0.0078$). Finally, using ImageJ we measured the area of individual mitochondria from electron micrographs from B6 control ($n = 6$) and TKO ($n = 6$) samples. We found that the average area of the mitochondria was increased in TKO eyes compared with B6 controls (Fig. 8F, $P = 0.035$). The

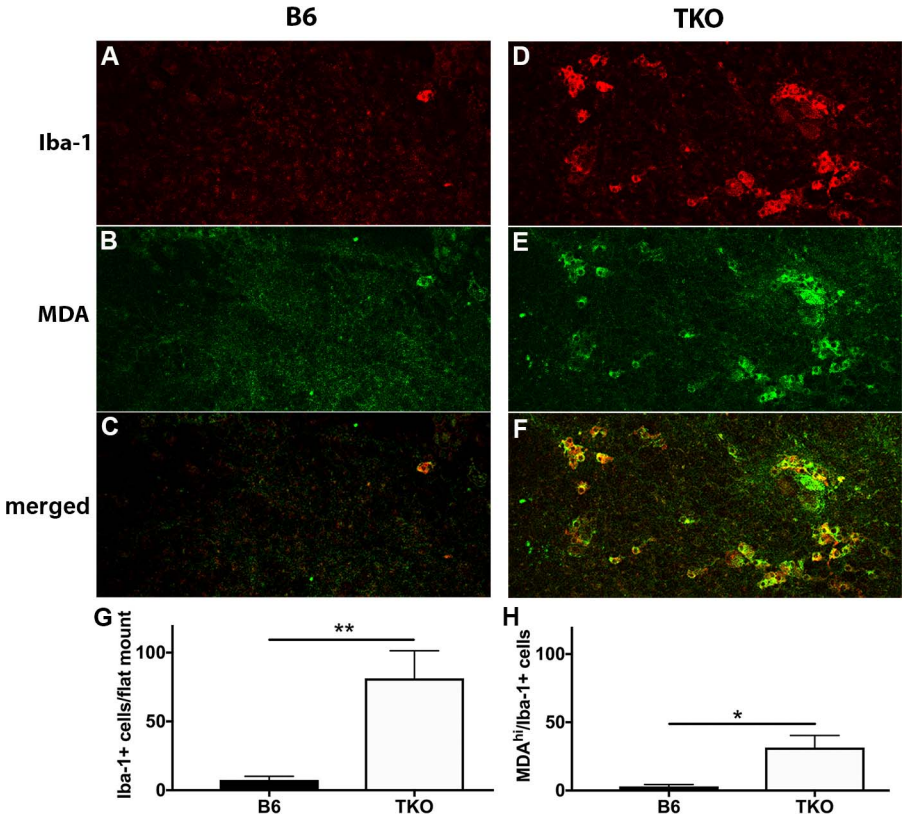

Figure 5. Increased subretinal microglia and retinal MDA accumulation in TKO mice. RPE–choroid–scleral flat mounts ("RPE flat mounts") of B6 controls (**A**–**C**) and TKO mice (**D**–**F**) were stained with Iba-1 and MDA and imaged by confocal microscopy. Eyes were collected from 13- to 16-month-old mice. Subretinal microglia showing staining for Iba-1+ (**A**, **D**) or MDA+ (**B**, **E**) are shown, as well as a merge of the two channels (**C**, **F**). A quantitative analysis of the data, showing the number of Iba-1+ microglia (**G**) and Iba-1+/MDA+ microglia (**H**) in both B6 control ($n = 8$) and TKO mice ($n = 11$) is shown. *Error bars* represent the standard error of the mean for experimental groups. The statistical significance was reported as $^{*}P < 0.05$, $^{**}P < 0.01$, $^{***}P < 0.001$.

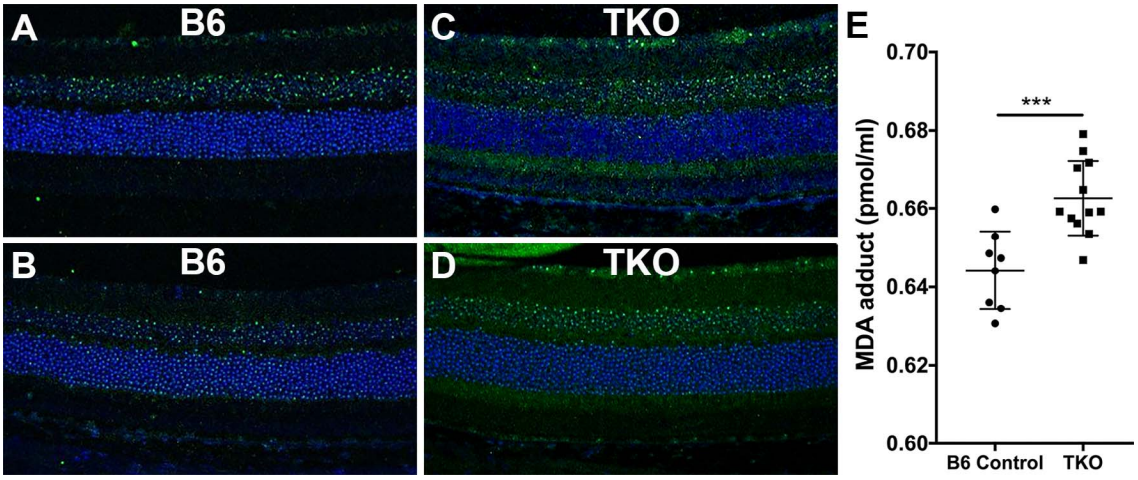

Figure 6. Increased retinal MDA-protein adducts in TKO mice. Eyes (4 per group) were collected for immunohistochemistry of retinal sections from 13- to 16-month-old B6 (**A**, **B**) and TKO (**C**, **D**) mice and probed with anti-MDA antibody. There is more MDA accumulation (green fluorescence) in eyes from TKO mice than eyes from B6 controls. Nuclei were stained with DAPI (*blue*). Retina samples were collected (**E**) from 13- to 16-month-old TKO ($n = 11$) and age- and sex-matched B6 controls ($n = 9$) mice and analyzed for MDA adduct content of retinal protein using an Oxiselect MDA adduct competitive ELISA Kit. TKO mice demonstrated a statistically significant increase in levels of retinal MDA-protein adducts compared with B6 controls. *Error bars* represent the standard error of the mean for experimental groups. The statistical significance was reported as $^{*}P < 0.05$, $^{**}P < 0.01$, $^{***}P < 0.001$.

Investigative Ophthalmology & Visual Science

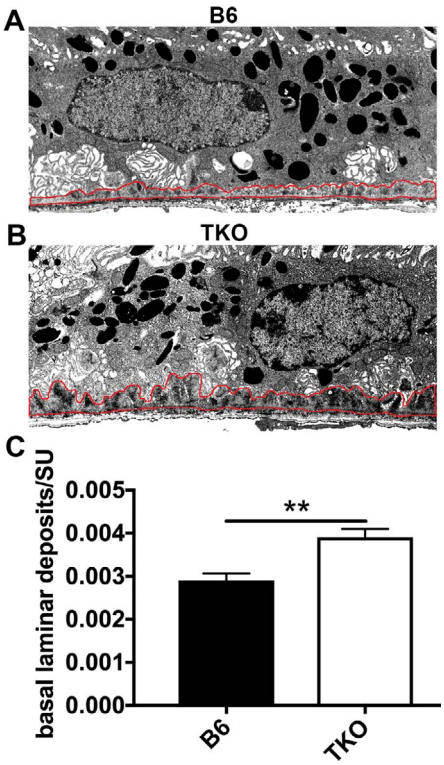

Figure 7. BLD are increased in aging TKO mice. Eyes were collected from 15-month-old B6 control (**A**, $n = 4$) and TKO (**B**, $n = 4$) mice for TEM. The accumulation of BLD under the RPE (**C**) was determined using the freehand tracing tool in ImageJ and reported as BLD in standard units. Approximately 40 TEM image fields (×2000 magnification) were measured and averaged per eye for BLD measurements. *Error bars* represent the standard error of the mean for experimental groups. The statistical significance was reported as $^{**}P < 0.01$.

mitochondria also appeared to be rounder in TKO samples compared with B6 controls (Figs. 8I, 8J versus 8G, 8H).

The Response of Scotopic Ganzfeld ERG Demonstrates Retinal Degeneration in Aging TKO Mice

Our next aim was to determine if the retinal and RPE abnormalities we had documented on exam, OCT images, immunostaining, ELISA, and electron microscopy correlated with changes on retinal function. We obtained scotopic Ganzfeld ERG measurements of a- and b-wave amplitudes in response to low- (0.1 log cd.s.m^{-2}) and high- (3.1 log cd.s.m^{-2}) flash intensities in eyes of age- and sex-matched TKO and B6 control mice (Fig. 9; Supplementary Fig. S2). At 6 months of age there was no difference between the two groups in either the a-wave or b-wave amplitudes (Figs. 9A, 9B, respectively). However, by 12 months of age there was a statistically significant decrease in a-wave amplitude in TKO mice compared with B6 control mice, and this was the case for both the low (Fig. 9A, $P = 0.0037$) and high-intensity stimuli (Fig. 9A, $P = 0.028$). This decrease in a-wave amplitude became more prominent at 15 months of age ($P = 0.0062$ for the low-intensity stimulus and $P = 0.0097$ for the high-intensity stimulus). Because most of the retinal changes we had documented seemed to affect the outer retina, we mostly expected changes in the a-wave of the ERG, which reflects the function of the outer retina (in particular, the photoreceptors). This was consistent with our findings. Although there was a trend toward a decrease in the amplitude of the b-wave both at 12 and 15 months, the difference was statistically significant only for the high-intensity stimulus at the 12-month time point (Fig. 9B, $P = 0.029$). The ERG changes indicate a significant loss in outer retinal function in aging TKO mice compared with B6 control mice.

Discussion

Chronic oxidative stress has been proposed to play an important role in many aging disorders, including AMD and neurodegenerative disorders. Modeling these disorders in the laboratory has been challenging, perhaps in part due to the short life span of mice. We hypothesized that mice with an increased level of chronic oxidative stress could provide a new platform on which to study aging disorders of the retina.

KO mice can provide a great deal of insight into mechanisms of disease. However, in nature, when a given gene or cellular process is targeted there is often an activation of compensatory pathways[22,37] due to the presence of redundant or alternative processes. SOD-1, Parkin, and DJ-1 are multifunctional proteins that play important roles in the oxidative stress response in neurodegenerative diseases, such as amyotrophic lateral sclerosis, Parkinson's disease, and Alzheimer's disease.[38] These three proteins also have been shown to be active in the retina and have been proposed to play a role in the protection of photoreceptors and RPE from oxidative damage.[10–15] Loss of function mutations in Parkin and Sod1 were found to share common mechanisms of actions. Previous studies reported that in addition to regulating the expression of Sod1, DJ-1 can also compensate for Sod1 when it is mutated,[20,21] demonstrating the complex interplay between these pathways. Finally, both DJ-1 and Sod1 interact with the Nrf2 pathway.[9] In our aging experiments, we used mice that are simultaneously deficient in superoxide *Sod1*, *Park7*, and *Prkn* (TKO mice) to try to circumvent the compensatory effects of these proteins. Even in the setting of TKO mice, a lack of enhanced neurodegeneration has been reported[22,39] perhaps due in part to additional compensatory mechanisms in the setting of a low-stress environment in the central nervous system with normal aging.[37] However, we hypothesized that the retina would be different, because it is highly susceptible to oxidative stress due to the following: (1) high exposure to light, (2) high oxygen levels, (3) high metabolic activity, and (4) high content of unsaturated fatty acids.

The earliest finding in the TKO mice was a change in the reflectivity of outer retinal layers on OCT that was consistently seen by 3 months of age. Following this, TKO mice develop, just with aging, an early accumulation of microglia in the subretinal space, which can be consistently seen by 6 months of age. Furthermore, these microglia stained positive for MDA, suggesting that they may have been activated or called in to help clear oxidative damage. We also demonstrated an increase in MDA-protein adducts in the retina of TKO mice, corroborating an increased level of retinal oxidative damage in these mice. This increased oxidative damage would likely explain our observation of early retinal structural deficits (retinal OCT reflectivity changes by 3 months of age, thinning on OCT by 5–6 months of age) and functional loss (decreased ERG amplitudes). Taken together these observations would suggest that the earliest changes in the TKO mice are happening at the outer retina level. However, further studies will be needed to better elucidate the early mechanisms of disease in this and other models of increased oxidative stress.

Our findings regarding ultrastructural changes in RPE cells suggest that chronic oxidative stress in the TKO mice is affecting not only the neural retina, but also the RPE. First, the

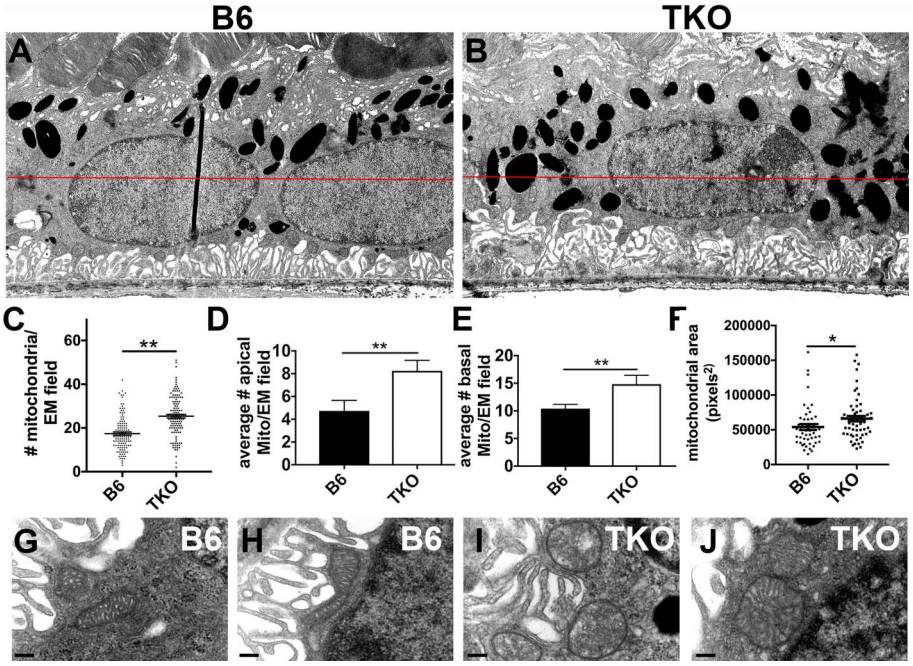

Figure 8. Mitochondria (Mito) numbers and relative size are increased in aging TKO mice. Eyes were collected from 15-month-old mice for TEM. Three B6 control (**A**) and four TKO (**B**) samples were included. Micrographs (×2000 magnification) or "EM fields" ($n = 120$ B6 control and 127 TKO) were analyzed in order to count the total number of mitochondria (**C**). We also classified mitochondria into apical (**D**) or basal (**E**). Finally, using ImageJ we measured the area of all mitochondria from an equal number of electron micrographs (×15,000 magnification) from B6 control ($n = 6$) and TKO ($n = 6$) samples. Because TKO RPE cells have more mitochondria per cell compared with B6 control mice, we ended up measuring the area of a total of 50 mitochondria for B6 control and 62 mitochondria for TKO. We found that the average area of the mitochondria was increased in TKO eyes compared with B6 controls (**F**). The mitochondria also appeared to be rounder in TKO samples compared with B6 controls (**I**, **J** versus **G**, **H**). *Error bars* represent the standard error of the mean for experimental groups. The statistical significance was reported as $^{*}P < 0.05$, $^{**}P < 0.01$.

increase in BLD is significant, because these deposits have been previously documented in multiple models of AMD and also after chronic oxidative stress.[1,29,40–47] The increased number of mitochondria indicate a disruption in metabolic homeostasis in RPE cells. Some studies[33] reported a decrease in the number of mitochondria in aging human retinas and retinas from AMD patients. However, recent studies suggest that in a setting in which mitochondria are damaged by oxidative stress[19] or in RPE from AMD donors,[48] there could be an increased accumulation of these organelles in the RPE. Several groups have shown that mice with increased oxidative stress develop an increased number and/or size of mitochondria in RPE cells, which seems to correlate with dysfunction.[34,49,50] In addition, a defect in Parkin may affect the elimination of depolarized/damaged mitochondria in cells exposed to oxidative stress (mitophagy).[16,19] Thus, although Parkin-independent mitophagy pathways exist,[51] it is possible that our findings in TKO mice are due to a combination of increased oxidative stress and defects in mitophagy.

Previously, we have shown that the TKO mice have increased susceptibility to light-induced oxidative stress.[23] The retinal structural attrition that we now document in the TKO mice in the current study without any exogenous oxidative stress application confirms that these antioxidant defense enzymes/proteins play important roles in the protection of the retina due to aging. Aging by itself is a risk factor in many of the neurodegenerative diseases, including AMD, and

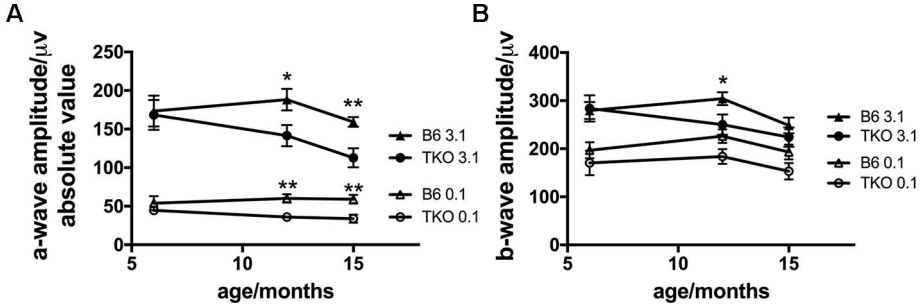

Figure 9. Aging TKO mice have decreased photoreceptor function compared with B6 controls. Scotopic Ganzfeld ERG a-wave (**A**) and b-wave (**B**) amplitudes were measured in response to low- (0.1 log cd.s.m^{-2}) and high- (3.1 log cd.s.m^{-2}) flash intensities in TKO and B6 control mice as a function of age. TKO mice demonstrated decreased a-wave amplitude both at 12 and 15 months of age. Each *symbol* represents mean values ± SEM for experimental groups. The following number of mice were analyzed for the 6-, 12-, and 15-month time points for each experimental group: B6 control = 7, 11, and 7, respectively; TKO = 4, 11, and 10, respectively. The statistical significance was reported as $^{*}P < 0.05$, $^{**}P < 0.01$.

these antioxidant enzymes/proteins protect the retina from cumulative oxidative damage.

Other mouse models of dry AMD show significant similarities and some differences when compared with the TKO mice. Zhao et al.[52] showed an accumulation of fundus spots in Nrf2 KO mice by 8 months of age compared with B6 controls and decreased ERG signals by 12 months of age. When Nrf2 KO mice were maintained on high-fat diet for 16 weeks they accumulated BLD starting at 11 months of age and showed increased accumulation of Iba-1–positive cells co-expressing the activation marker CD68.[53] Manipulation of complement factor H has also resulted in a milder form of some of the changes that we describe in TKO mice. The Bowes-Rickman Lab described increased sub-RPE deposits (BLD) in old Cfh+/– and Cfh–/– mice fed high-fat, high-cholesterol diet (HFC).[41] Their Cfh+/v mice also show functional deficits by approximately 22 to 27 months of age (91–110 weeks) when fed the HFC diet for 8 weeks. Working with complement factor-H transgenic mice, both the Rickman group[54] and our group[1] found an increased accumulation of BLD under the RPE, which is recognized as an important disease parameter in aging mouse models of AMD-like pathology.[1,29,40–47] Interestingly, our TKO mice show similar and, in some cases, more severe pathology than that reported in these important models without exogenous stressors, such as high-fat diet. We have not seen a reported analysis of outer retina reflectivity changes in these models, but it is interesting that we can document a statistically significant change in TKO mice that is obvious on plain inspection of OCT images by 3 months of age.

Targeting mitochondrial function in RPE cells (via the mitochondrial superoxide dismutase *Sod2* or the mitochondrial transcription factor A "*Tfam*") can also lead to oxidative stress and to pathology similar to what we describe in the TKO mice. Using RPE-specific *Sod2*-knockdown mice (generated by subretinal AAV-Rz432 injection), the Lewin group[55] found a reduction in a- and b-waves 3 to 6 months postinjection (at 9–12 months of age). These mice also had thinning of the ONL on spectral-domain OCT (12 months postinjection) and BM and mitochondrial abnormalities on EM (7 months postinjection). They corroborated some of these findings using a conditional knockdown of *Sod2* in the RPE layer.[56] Similarly, RPE-specific *Tfam* KO mice developed diminished oxidative phosphorylation capacity and mitochondrial enlargement.[49] These mice also showed thinning of the ONL, decreased ERG responses (a- and b-waves) at 36 weeks of age.

One caveat to our study, as with all mouse models of human disease, is how species-specific differences could affect the findings. In our case, one factor that comes to mind is the recruitment of subretinal microglia. Subretinal microglia/macrophages have been described in humans, particularly in specimens from patients with different stages of AMD.[57–59] However, the recruitment of subretinal microglia appears to be more prominent in the mouse than in humans. Although some studies suggest that these cells promote disease progression (perhaps by secreting proinflammatory or proangiogenic factors),[60–62] it is possible that in some settings they could be protective (by clearing proinflammatory debris).[60,63–65] Thus, the jury is still out on whether in many mouse models these subretinal microglia may prevent the development of more AMD-specific findings like drusen or choroidal neovascularization. A second caveat is that a direct comparison of our TKO mice with individual, single KO mice has not been made. Based on analysis of the literature it seems that TKO mice may start accumulating subretinal microglia earlier than the single KO mice; a significant difference in the accumulation of white fundus spots is seen by 6 months of age in the TKO mice versus 10 months for the *Sod1* KO mice.[3] We also suspect that retinal changes in TKO mice are more prominent than in DJ-$1^{-/-}$,[11] and Parkin$^{-/-}$,[17] mice and at least as prominent as those seen in *Sod1*$^{-/-}$.[14] In particular, retinal thinning appears to occur sometime between 6 and 9 months of age. However, side-to-side comparisons would be helpful. For example, we describe early qualitative and quantitative differences in the outer retinal layers of TKO mice by 3 months of age. It would be helpful to determine using the same techniques how this compares with single KO mice. More importantly, it is possible that more pronounced differences between TKO mice and the single KO mice may surface when the different models are exposed to stressors (e.g., light-induced retinal degeneration, which we have shown is markedly increased in TKO mice).[23]

Given the demonstrated increased oxidative stress and the early structural changes observed, we propose that the TKO mice can serve as a platform to study retinal diseases that involve chronic oxidative stress, including macular degeneration,[11] retinal detachment,[66,67] and ischemic retinopathies.[68] To model each of these diseases, additional disease-specific facilitators or triggers (e.g., genes, experimental retinal detachment, and ischemia) could be superimposed onto the TKO mice. Such studies could provide better insight into disease mechanisms and perhaps lead to new therapeutic approaches.

Acknowledgments

Supported by National Institutes of Health Grant 1R01EY022652 (Bethesda, MD, USA), Visual Science Core Grant EY020799 (Bethesda, MD, USA), an unrestricted grant from Research to Prevent Blindness (New York, NY, USA), the Patricia and Col. William Massad Retina Research Fund (Dallas, TX, USA), and a grant from the David M. Crowley Foundation (Dallas, TX, USA).

Disclosure: **Y. Zhu**, None; **B. Aredo**, None; **B. Chen**, None; **C.X. Zhao**, None; **Y.-G. He**, None; **R.L. Ufret-Vincenty**, None

References

1. Aredo B, Li T, Chen X, et al. A chimeric Cfh transgene leads to increased retinal oxidative stress, inflammation, and accumulation of activated subretinal microglia in mice. *Invest Ophthalmol Vis Sci*. 2015;56:3427–3440.
2. Hollyfield JG, Bonilha VL, Rayborn ME, et al. Oxidative damage-induced inflammation initiates age-related macular degeneration. *Nat Med*. 2008;14:194–198.
3. Imamura Y, Noda S, Hashizume K, et al. Drusen, choroidal neovascularization, and retinal pigment epithelium dysfunction in SOD1-deficient mice: a model of age-related macular degeneration. *Proc Natl Acad Sci U S A*. 2006;103:11282–11287.
4. Rohrer B, Bandyopadhyay M, Beeson C. Reduced metabolic capacity in aged primary retinal pigment epithelium (RPE) is correlated with increased susceptibility to oxidative stress. *Adv Exp Med Biol*. 2016;854:793–798.
5. Shaw PX, Zhang L, Zhang M, et al. Complement factor H genotypes impact risk of age-related macular degeneration by interaction with oxidized phospholipids. *Proc Natl Acad Sci U S A*. 2012;109:13757–13762.
6. Shen JK, Dong A, Hackett SF, Bell WR, Green WR, Campochiaro PA. Oxidative damage in age-related macular degeneration. *Histol Histopathol*. 2007;22:1301–1308.
7. Weismann D, Hartvigsen K, Lauer N, et al. Complement factor H binds malondialdehyde epitopes and protects from oxidative stress. *Nature*. 2011;478:76–81.
8. Campochiaro PA, Strauss RW, Lu L, et al. Is there excess oxidative stress and damage in eyes of patients with retinitis pigmentosa? *Antioxid Redox Signal*. 2015;23:643–648.
9. Milani P, Ambrosi G, Gammoh O, Blandini F, Cereda C. SOD1 and DJ-1 converge at Nrf2 pathway: a clue for antioxidant

therapeutic potential in neurodegeneration. *Oxid Med Cell Longev*. 2013;2013:836760.

10. Bonilha VL, Bell BA, Rayborn ME, et al. Loss of DJ-1 elicits retinal abnormalities, visual dysfunction, and increased oxidative stress in mice. *Exp Eye Res*. 2015;139:22–36.
11. Bonilha VL, Bell BA, Rayborn ME, et al. Absence of DJ-1 causes age-related retinal abnormalities in association with increased oxidative stress. *Free Radic Biol Med*. 2017;104:226–237.
12. Dong A, Shen J, Krause M, et al. Superoxide dismutase 1 protects retinal cells from oxidative damage. *J Cell Physiol*. 2006;208:516–526.
13. Esteve-Rudd J, Campello L, Herrero MT, Cuenca N, Martín-Nieto J. Expression in the mammalian retina of parkin and UCH-L1, two components of the ubiquitin-proteasome system. *Brain Res*. 2010;1352:70–82.
14. Hashizume K, Hirasawa M, Imamura Y, et al. Retinal dysfunction and progressive retinal cell death in SOD1-deficient mice. *Am J Pathol*. 2008;172:1325–1331.
15. Shadrach KG, Rayborn ME, Hollyfield JG, Bonilha VL. DJ-1-dependent regulation of oxidative stress in the retinal pigment epithelium (RPE). *PLoS One*. 2013;8:e67983.
16. Brennan L, Khoury J, Kantorow M. Parkin elimination of mitochondria is important for maintenance of lens epithelial cell ROS levels and survival upon oxidative stress exposure. *Biochim Biophys Acta*. 2017;1863:21–32.
17. Palacino JJ, Sagi D, Goldberg MS, et al. Mitochondrial dysfunction and oxidative damage in parkin-deficient mice. *J Biol Chem*. 2004;279:18614–18622.
18. Yang YX, Muqit MM, Latchman DS. Induction of parkin expression in the presence of oxidative stress. *Eur J Neurosci*. 2006;24:1366–1372.
19. Hu X, Dai Y, Sun X. Parkin overexpression protects retinal ganglion cells against glutamate excitotoxicity. *Mol Vis*. 2017;23:447–456.
20. Wang Z, Liu J, Chen S, et al. DJ-1 modulates the expression of Cu/Zn-superoxide dismutase-1 through the Erk1/2-Elk1 pathway in neuroprotection. *Ann Neurol*. 2011;70:591–599.
21. Yamashita S, Mori A, Kimura E, et al. DJ-1 forms complexes with mutant SOD1 and ameliorates its toxicity. *J Neurochem*. 2010;113:860–870.
22. Hennis MR, Seamans KW, Marvin MA, Casey BH, Goldberg MS. Behavioral and neurotransmitter abnormalities in mice deficient for Parkin, DJ-1 and superoxide dismutase. *PLoS One*. 2013;8:e84894.
23. Ding Y, Aredo B, Zhong X, Zhao CX, Ufret-Vincenty RL. Increased susceptibility to fundus camera-delivered light-induced retinal degeneration in mice deficient in oxidative stress response proteins. *Exp Eye Res*. 2017;159:58–68.
24. Luhmann UF, Robbie S, Munro PM, et al. The drusenlike phenotype in aging Ccl2-knockout mice is caused by an accelerated accumulation of swollen autofluorescent subretinal macrophages. *Invest Ophthalmol Vis Sci*. 2009;50:5934–5943.
25. Mattapallil MJ, Wawrousek EF, Chan CC, et al. The Rd8 mutation of the Crb1 gene is present in vendor lines of C57BL/6N mice and embryonic stem cells, and confounds ocular induced mutant phenotypes. *Invest Ophthalmol Vis Sci*. 2012;53:2921–2927.
26. Elchuri S, Oberley TD, Qi W, et al. CuZnSOD deficiency leads to persistent and widespread oxidative damage and hepatocarcinogenesis later in life. *Oncogene*. 2005;24:367–380.
27. Muller FL, Song W, Liu Y, et al. Absence of CuZn superoxide dismutase leads to elevated oxidative stress and acceleration of age-dependent skeletal muscle atrophy. *Free Radic Biol Med*. 2006;40:1993–2004.
28. Zhong X, Aredo B, Ding Y, Zhang K, Zhao CX, Ufret-Vincenty RL. Fundus camera-delivered light-induced retinal degeneration in mice with the RPE65 Leu450Met variant is associated with oxidative stress and apoptosis. *Invest Ophthalmol Vis Sci*. 2016;57:5558–5567.
29. Ufret-Vincenty RL, Aredo B, Liu X, et al. Transgenic mice expressing variants of complement factor H develop AMD-like retinal findings. *Invest Ophthalmol Vis Sci*. 2010;51:5878–5887.
30. Aredo B, Zhang K, Chen X, Wang CX, Li T, Ufret-Vincenty RL. Differences in the distribution, phenotype and gene expression of subretinal microglia/macrophages in C57BL/6N (Crb1 rd8/rd8) versus C57BL6/J (Crb1 wt/wt) mice. *J Neuroinflammation*. 2015;12:6.
31. Raoul W, Feumi C, Keller N, et al. Lipid-bloated subretinal microglial cells are at the origin of drusen appearance in CX3CR1-deficient mice. *Ophthalmic Res*. 2008;40:115–119.
32. Chen X, Kezic J, Bernard C, McMenamin PG. Rd8 mutation in the Crb1 gene of CD11c-eYFP transgenic reporter mice results in abnormal numbers of CD11c-positive cells in the retina. *J Neuropathol Exp Neurol*. 2013;72:782–790.
33. Feher J, Kovacs I, Artico M, Cavallotti C, Papale A, Balacco Gabrieli C. Mitochondrial alterations of retinal pigment epithelium in age-related macular degeneration. *Neurobiol Aging*. 2006;27:983–993.
34. Gautier CA, Kitada T, Shen J. Loss of PINK1 causes mitochondrial functional defects and increased sensitivity to oxidative stress. *Proc Natl Acad Sci U S A*. 2008;105:11364–11369.
35. Bianchi E, Scarinci F, Ripandelli G, et al. Retinal pigment epithelium, age-related macular degeneration and neurotrophic keratouveitis. *Int J Mol Med*. 2013;31:232–242.
36. Toms M, Burgoyne T, Tracey-White D, et al. Phagosomal and mitochondrial alterations in RPE may contribute to KCNJ13 retinopathy. *Sci Rep*. 2019;9:3793.
37. Schneider JL, Villarroya J, Diaz-Carretero A, et al. Loss of hepatic chaperone-mediated autophagy accelerates proteostasis failure in aging. *Aging Cell*. 2015;14:249–264.
38. Bonifati V, Rizzu P, van Baren MJ, et al. Mutations in the DJ-1 gene associated with autosomal recessive early-onset parkinsonism. *Science*. 2003;299:256–259.
39. Kitada T, Tong Y, Gautier CA, Shen J. Absence of nigral degeneration in aged parkin/DJ-1/PINK1 triple knockout mice. *J Neurochem*. 2009;111:696–702.
40. Rowan S, Weikel K, Chang ML, et al. Cfh genotype interacts with dietary glycemic index to modulate age-related macular degeneration-like features in mice. *Invest Ophthalmol Vis Sci*. 2014;55:492–501.
41. Toomey CB, Kelly U, Saban DR, Bowes Rickman C. Regulation of age-related macular degeneration-like pathology by complement factor H. *Proc Natl Acad Sci U S A*. 2015;112:E3040–E3049.
42. Handa JT, Tagami M, Ebrahimi K, et al. Lipoprotein (A) with An intact lysine binding site protects the retina from an age-related macular degeneration phenotype in mice (an American Ophthalmological Society Thesis). *Trans Am Ophthalmol Soc*. 2015;113:T5.
43. Hu P, Herrmann R, Bednar A, et al. Aryl hydrocarbon receptor deficiency causes dysregulated cellular matrix metabolism and age-related macular degeneration-like pathology. *Proc Natl Acad Sci U S A*. 2013;110:E4069–E4078.
44. Marin-Castaño ME, Striker GE, Alcazar O, Catanuto P, Espinosa-Heidmann DG, Cousins SW. Repetitive nonlethal oxidant injury to retinal pigment epithelium decreased extracellular matrix turnover in vitro and induced sub-RPE deposits in vivo. *Invest Ophthalmol Vis Sci*. 2006;47:4098–4112.
45. Espinosa-Heidmann DG, Suner IJ, Catanuto P, Hernandez EP, Marin-Castano ME, Cousins SW. Cigarette smoke-related oxidants and the development of sub-RPE deposits in an

Investigative Ophthalmology & Visual Science

experimental animal model of dry AMD. *Invest Ophthalmol Vis Sci*. 2006;47:729–737.

46. Fujihara M, Nagai N, Sussan TE, Biswal S, Handa JT. Chronic cigarette smoke causes oxidative damage and apoptosis to retinal pigmented epithelial cells in mice. *PLoS One*. 2008;3: e3119.
47. Cousins SW, Espinosa-Heidmann DG, Alexandridou A, Sall J, Dubovy S, Csaky K. The role of aging, high fat diet and blue light exposure in an experimental mouse model for basal laminar deposit formation. *Exp Eye Res*. 2002;75:543–553.
48. Ferrington DA, Sinha D, Kaarniranta K. Defects in retinal pigment epithelial cell proteolysis and the pathology associated with age-related macular degeneration. *Prog Retin Eye Res*. 2016;51:69–89.
49. Zhao C, Yasumura D, Li X, et al. mTOR-mediated dedifferentiation of the retinal pigment epithelium initiates photoreceptor degeneration in mice. *J Clin Invest*. 2011;121:369–383.
50. Brown EE, DeWeerd AJ, Ildefonso CJ, Lewin AS, Ash JD. Mitochondrial oxidative stress in the retinal pigment epithelium (RPE) led to metabolic dysfunction in both the RPE and retinal photoreceptors. *Redox Biol*. 2019;24:101201.
51. Villa E, Marchetti S, Ricci JE. No Parkin zone: mitophagy without Parkin. *Trends Cell Biol*. 2018;28:882–895.
52. Zhao Z, Chen Y, Wang J, et al. Age-related retinopathy in NRF2-deficient mice. *PLoS One*. 2011;6:e19456.
53. Zhao Z, Xu P, Jie Z, et al. γδ T cells as a major source of IL-17 production during age-dependent RPE degeneration. *Invest Ophthalmol Vis Sci*. 2014;55:6580–6589.
54. Landowski M, Kelly U, Klingeborn M, et al. Human complement factor H Y402H polymorphism causes an age-related macular degeneration phenotype and lipoprotein dysregulation in mice. *Proc Natl Acad Sci U S A*. 2019;116: 3703–3711.
55. Seo SJ, Krebs MP, Mao H, Jones K, Conners M, Lewin AS. Pathological consequences of long-term mitochondrial oxidative stress in the mouse retinal pigment epithelium. *Exp Eye Res*. 2012;101:60–71.
56. Biswal MR, Ildefonso CJ, Mao H, et al. Conditional induction of oxidative stress in RPE: a mouse model of progressive retinal degeneration. *Adv Exp Med Biol*. 2016;854:31–37.
57. Grossniklaus HE, Miskala PH, Green WR, et al. Histopathologic and ultrastructural features of surgically excised subfoveal choroidal neovascular lesions: submacular surgery trials report no. 7. *Arch Ophthalmol*. 2005;123:914–921.
58. Gupta N, Brown KE, Milam AH. Activated microglia in human retinitis pigmentosa, late-onset retinal degeneration, and age-related macular degeneration. *Exp Eye Res*. 2003;76:463–471.
59. Combadière C, Feumi C, Raoul W, et al. CX3CR1- dependent subretinal microglia cell accumulation is associated with cardinal features of age-related macular degeneration. *J Clin Invest*. 2007;117:2920–2928.
60. Kelly J, Ali Khan A, Yin J, Ferguson TA, Apte RS. Senescence regulates macrophage activation and angiogenic fate at sites of tissue injury in mice. *J Clin Invest*. 2007;117:3421–3426.
61. Espinosa-Heidmann DG, Suner IJ, Hernandez EP, Monroy D, Csaky KG, Cousins SW. Macrophage depletion diminishes lesion size and severity in experimental choroidal neovascularization. *Invest Ophthalmol Vis Sci*. 2003;44:3586–3592.
62. Cousins SW, Espinosa-Heidmann DG, Csaky KG. Monocyte activation in patients with age-related macular degeneration: a biomarker of risk for choroidal neovascularization? *Arch Ophthalmol*. 2004;122:1013–1018.
63. Ng TF, Streilein, JW. Light-induced migration of retinal microglia into the subretinal space. *Invest Ophthalmol Vis Sci*. 2001;42:3301–3310.
64. Ambati J, Anand A, Fernandez S, et al. An animal model of age-related macular degeneration in senescent Ccl-2- or Ccr-2-deficient mice. *Nat Med*. 2003;9:1390–1397.
65. Apte RS, Richter J, Herndon J, Ferguson TA. Macrophages inhibit neovascularization in a murine model of age-related macular degeneration. *PLoS Med*. 2006;3:e310.
66. Ghosh F, Åkerström B, Bergwik J, Abdshill H, Gefors L, Taylor L. Acute tissue reactions, inner segment pathology, and effects of the antioxidant α1-microglobulin in an in vitro model of retinal detachment. *Exp Eye Res*. 2018;173:13–23.
67. Cederlund M, Ghosh F, Arnér K, Andréasson S, Akerström B. Vitreous levels of oxidative stress biomarkers and the radical-scavenger α1-microglobulin/A1M in human rhegmatogenous retinal detachment. *Graefes Arch Clin Exp Ophthalmol*. 2013;251:725–732.
68. Rivera JC, Dabouz R, Noueihed B, Omri S, Tahiri H, Chemtob S. Ischemic retinopathies: oxidative stress and inflammation. *Oxid Med Cell Longev*. 2017;2017:3940241.

Investigative Ophthalmology & Visual Science